PHYSICAL REVIEW B VOLUME 61, NUMBER 19 15 MAY 2000-I

Electronic structure and bonding properties of layered machinable Ti_2AlC and Ti_2AlN ceramics

Yanchun Zhou and Zhimei Sun
Ceramic and Composite Department, Institute of Metal Research, Chinese Academy of Sciences, 72 Wenhua Road, Shenyang 110015, People's Republic of China

(Received 27 May 1999; revised manuscript received 23 August 1999)

The electronic structure and chemical bonding of the layered ternary compounds Ti_2AlC and Ti_2AlN have been calculated by the *ab initio* pseudopotential total-energy method. The results show that Ti_2AlC and Ti_2AlN exhibit metallic electrical conductivity with an anisotropic character and Ti_2AlC should be more conductive than Ti_2AlN. The chemical bonding in Ti_2AlC and Ti_2AlN is also anisotropic and is metallic-covalent-ionic in nature. On the basis of total-energy estimation we conclude that the replacement of C by N will result in a stabilization of the hexagonal structure and decrease in metallic properties.

Recently, a new family of layered machinable ceramics called H phases has shown unique properties that are attractive to both material scientists and physicists.[1–8] The salient properties of this new family of ceramics are high melting point, high strength and modulus, damage tolerance at room temperature, high thermal and electrical conductivity, good high-temperature-oxidation resistance, and machinable by both electrical discharge method and conventional cutting tools. The H phases are hexagonal complex ternary compounds with a common formula of M_2BX, where M is a transition metal. B is a group B element, and X is either carbon or nitrogen. Ti_2AlC and Ti_2AlN are two interesting materials from this family. Polycrystalline Ti_2AlC and Ti_2AlN ceramics have been fabricated by Barsoum, Brodkin, and El-Raghy[1] using a hot pressing method. Their work has demonstrated that Ti_2AlC and Ti_2AlN have excellent machinability, hardness of 3–6 GPa, electrical conductivity in the range of $2-5\times10^6\,\Omega^{-1}\,\mathrm{m}^{-1}$, high yield strength, and significant plasticity at high temperatures. These properties are believed to be strongly related to the structural properties and we are intrigued with establishing the relations between them. In this paper, we investigate the electronic structure and bonding properties of Ti_2AlC and Ti_2AlN compounds by means of the *ab initio* calculation. Our calculation will give a better picture of electronic structure and bonding properties for Ti_2AlC and Ti_2AlN. The purpose of this work is to understand: (i) Why they are conductive? What is the reason for the electronic transport properties in Ti_2AlC and Ti_2AlN? (ii) Why do the compounds, i.e., Ti_2AlC and Ti_2AlN, adopt the structures they have and how their physical properties are related to their crystal and electronic structures? The eventual goal will be useful in predicting the structures and properties of new materials.

The calculations are based on the *ab initio* pseudopotential total-energy method,[9] with the electron states being expanded in a plane-wave basis, and the energy minimization with respect to the plane-wave coefficients being carried out using the local-density approximation (LDA).[10,11] We use Perdew and Zunger's parametrization[12] for the exchange-correlation energy and seperable norm-conserving Kerker pseudopetentials[13] in the Kleinman-Bylander form.[14] The nonlocal potentials are treated in real space, using the method proposed by King-Smith, Payne, and Lin.[15]

Ti_2AlC and Ti_2AlN crystallize in the Cr_2AlC-type structure[16] with the $P6_3/mmc$[17,18] space group and Ti at $(4f)$, Al at $(2c)$ and C at $(2a)$ Wyckoff positions. The hexagonal lattice constants are $a=3.04$ Å, $c=13.60$ Å for Ti_2AlC, and $a=2.99$ Å, $c=13.61$ Å for Ti_2AlN. Figures 1(a) and 1(b) show the crystal structure of Ti_2AlC and Ti_2AlN, respectively. And the corresponding Brillouin zone is depicted in Fig. 1(c).

I. Ti_2AlC

The calculated band structure and its corresponding total density of states for Ti_2AlC are given in Figs. 2(a) and 2(b).

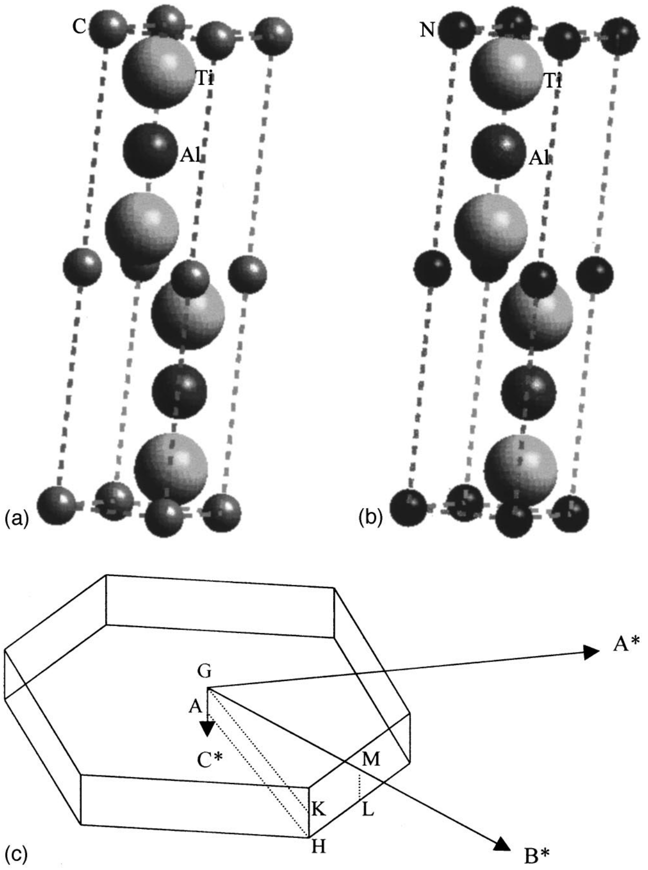

FIG. 1. (a) Crystal structure of Ti_2AlC, (b) crystal structure of Ti_2AlN, (c) the Brillouin zone and high-symmetry points for hexagonal Ti_2AlC and Ti_2AlN.

0163-1829/2000/61(19)/12570(4)/$15.00 PRB 61

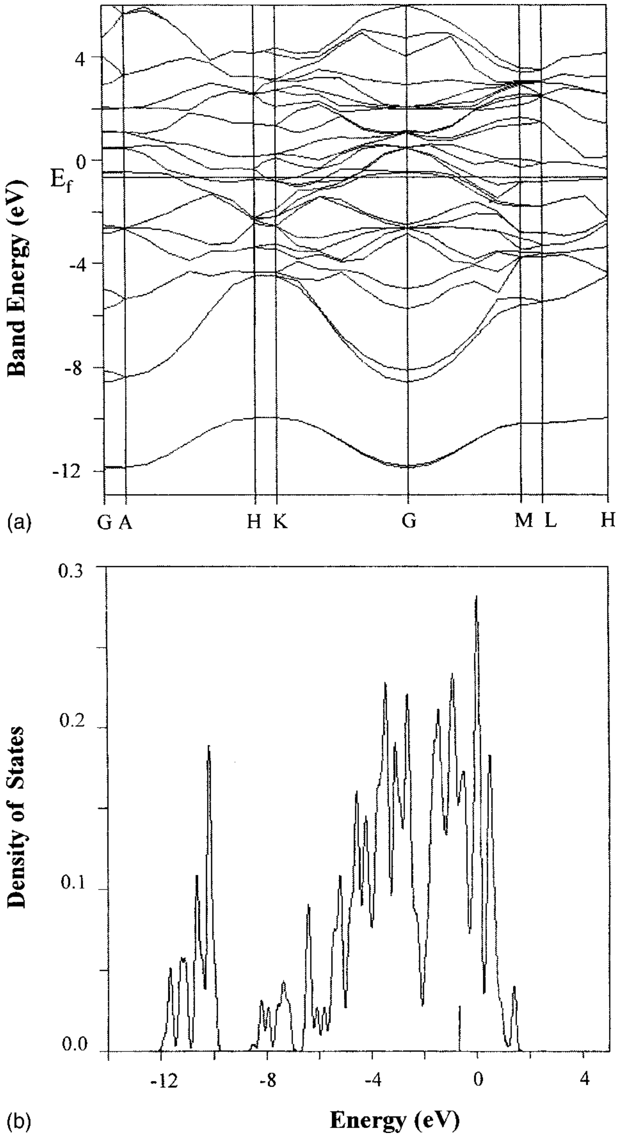

FIG. 2. (a) The calculated band structure of Ti_2AlC, and (b) total density of states for Ti_2AlC.

It is seen that there is no band gap at the Fermi level and the density of states (DOS) at which is 0.17 states/eV per unit cell. Valence and conduction bands overlap significantly at Fermi level. As a result, Ti_2AlC will exhibit metallic properties, such as metallic electrical and thermal conductivity, which agrees well with the experimental results of Barsoum, Brodkin, and El-Raghy.[1] Note that the energy gap between (Al, C) *s* and (Al, C) *p* for Ti_2AlC is relatively small: the indirect gap is about 1 eV, which implies the *sp* hybidization.

The band structure also shows strongly anisotropic features with less *c*-axis energy dispersion [see Fig. 2(a) in which there is much less energy dispersion along the short *H*-*K* and *M*-*L* directions]. Consequently, the electrical conductivity is anisotropic for single crystal Ti_2AlC, i.e., the electrical conductivity along the *c*-axis is much lower than that in the basal planes.

The metallic properties of Ti_2AlC and its anisotropic characteristics can also be directly seen in Fig. 3, where the distribution of charge density on different planes is shown. Figs. 3(a), 3(b), and 3(c) are distributions of charge density in

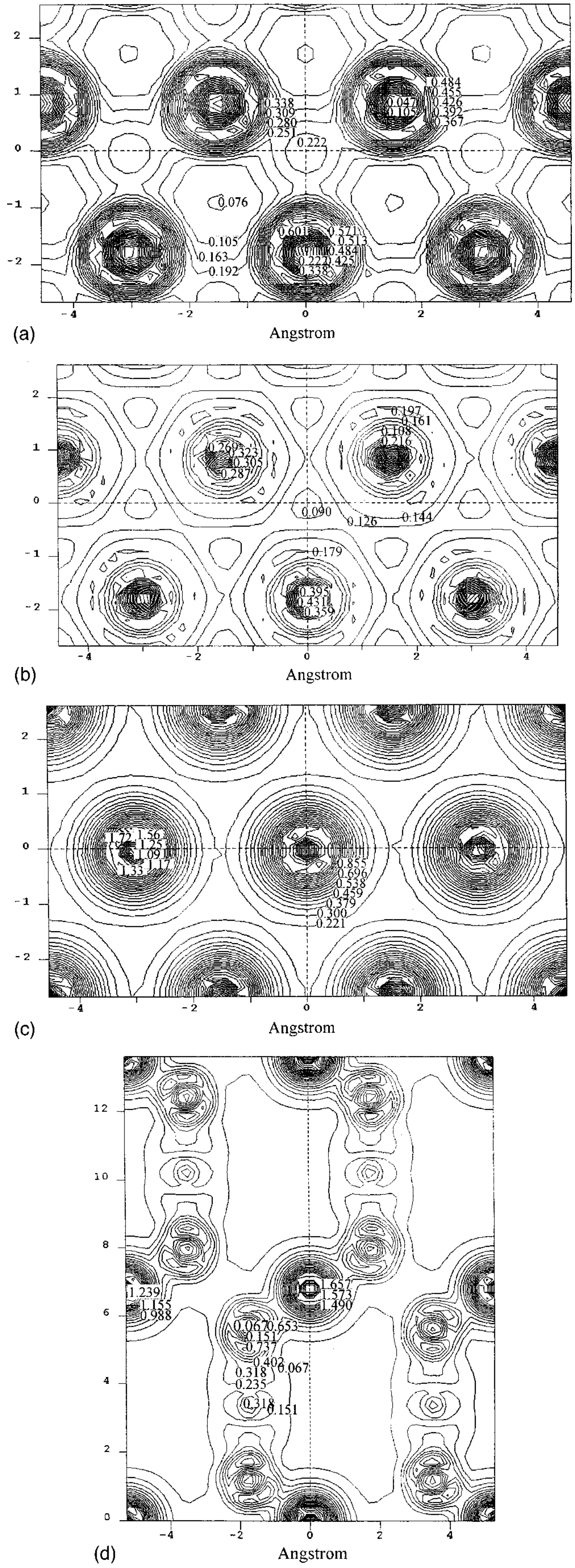

FIG. 3. Distribution of charge density on (a) Ti, (b) Al, (c) C atomic layers that are parallel to the basal plane, and on the (110) plane (d) of Ti_2AlC.

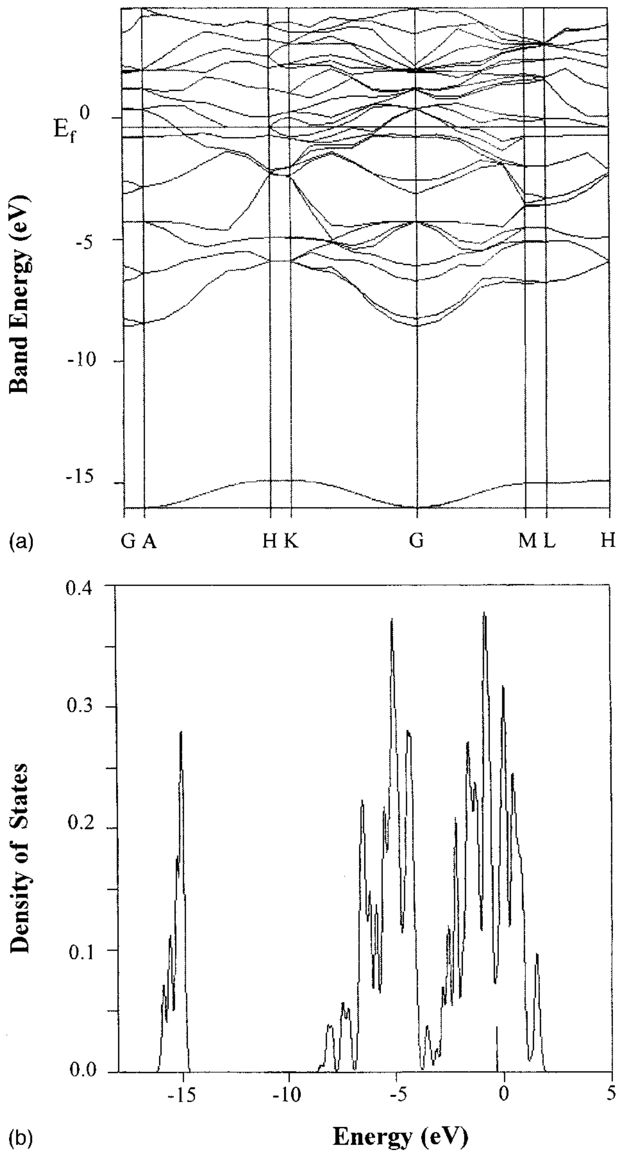

FIG. 4. (a) The calculated band structure, and (b) total density of states for Ti_2AlN.

atomic layers of Ti, Al, and C that are parallel to the basal plane, and Fig. 3(d) is the distribution of charge density on (110) plane of Ti_2AlC. For the convenience of discussion, a $2\times2\times1$ cell was used in Fig. 3. It is obvious to see from Fig. 3 that there is metallic bonding in Ti and Al layers, while there is no free charge density distribution in C planes. In the (110) plane, the charge density distribution gives detailed information on the interaction between different atoms. The Ti-C interaction in Ti_2AlC is covalent in nature and is very strong. At the same time, the more electronegative nature of C compared to Ti confirms the presence of ionic bonding between Ti and C, while the more electropositive nature of Al confirms the ionic bonding between Ti and Al. Therefore, the chemical bonding in Ti_2AlC is metallic-covalent-ionic in nature. The covalent component is due to the local interactions of hybridized (Ti, Al)d and C $2p$ states. Again the chemical bonding in Ti_2AlC is anisotropy with metallic bonding in Ti and Al layers that are parallel to the basal plane, whereas strong directional covalent and ionic bonding are between Ti-C and Ti-Al atoms. This strong an-

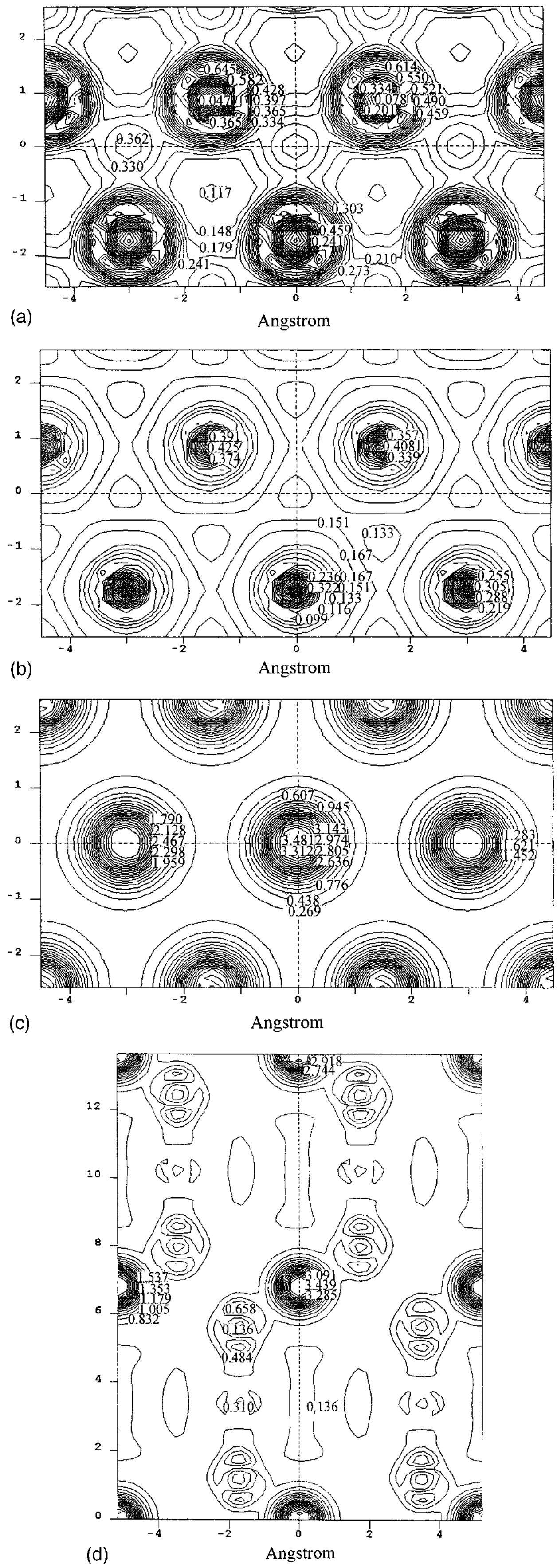

FIG. 5. Distribution of charge density on (a) Ti, (b) Al, (c) N atomic layers that are parallel to the basal plane, and on the (110) plane (d) of Ti_2AlN.

isotropy of chemical bonding is related to the physical and mechanical properties of the layered materials. High melting points and modulus are expected from the strong covalent and ionic bonding, while good electrical conductivity and microscale plasticity are expected from the existence of metallic bonding.

II. Ti_2AlN

Figures 4(a) and 4(b) show the electronic band structure and its corresponding total density of states. Note that the replacement of N for C results in the decrease in the DOS at Fermi level, which is 0.07 states eV per unit cell for Ti_2AlN. The energy gap between (Al, N) *s* and (Al, N) *p* states is much larger than that of (Al, C): the indirect energy gap is 6.2 eV, indicating that there is no or less *sp* hybridization in Ti_2AlN. The valence bands below Fermi level are similar to that of Ti_2AlC. No energy gap appears at the Fermi level; valence and conduction bands overlap with considerable anisotropic character. There is less energy dispersion along the short H-K and M-L directions compared to the dispersion normal to the *c*-axis. Consequently, Ti_2AlN will also exhibit anisotropic metallic properties. It shows metallic electrical conductivity parallel to the basal plane, while that along the *c* axis is much weaker. Barsoum, Brodkin, and El-Raghy[1] reported that the electrical conductivity for polycrystalline Ti_2AlC was $2.8\times10^6\ \Omega^{-1}\,\mathrm{m}^{-1}$ and that for Ti_2AlN was $3.2\times10^6\ \Omega^{-1}\,\mathrm{m}^{-1}$. Comparing the band structure and density of states of Fig. 2 for Ti_2AlC and Fig. 4 for Ti_2AlN, we assume that Ti_2AlC should be more conductive than Ti_2AlN in the basal plane.

It is also interesting to note that the Fermi level lies in a dip of DOS for Ti_2AlN, which reduces the band-structure energy and often correlates to the structure stability. Further, the total energy for Ti_2AlN is -1040.92 eV, while that for Ti_2AlC it is -804.71 eV indicating that Ti_2AlN is more stable than Ti_2AlC.

Figs. 5(a), 5(b), and 5(c) show the charge density distribution in Ti, Al, and N atomic layers that are parallel to the basal plane, and Fig. 5(d) gives the charge density distribution on the (110) plane. The charge density distributions in Ti layer and Al layer show metallic bonding between Ti-Ti, and Al-Al in atomic layers that are parallel to the basal plane. In the (110) plane, however, there is stronger ionic bonding between Ti-N in Ti_2AlN, while the covalent bonding between Ti-N is relatively weaker. Ionic bonding is formed between Ti-Al for Ti_2AlN, which is obvious from the much higher electron positive for Al than that for Ti. This conclusion agrees well with the analysis in Sec. I, i.e., there is much larger energy gap between (Al, N) *s* and *p* states for Ti_2AlN than that between (Al, C) *s* and *p* states for Ti_2AlC, implying that there is (Al, C) *sp* hybridization in Ti_2AlC, whereas less or no *sp* hybridization in Ti_2AlN. The *sp* hybridization leads to the increase in covalent bonding from Ti_2AlN to Ti_2AlC. Therefore, Ti_2AlN demonstrates similar anisotropic chemical bonding to Ti_2AlC. The chemical bonding is metallic-covalent-ionic in nature with more contribution from ionic and metallic bond, which will result in the anisotropic properties in Ti_2AlN.

We studied the electronic structure and chemical bonding of the hexagonal Ti_2AlC and Ti_2AlN compounds using the total-energy pseudopotential method. Our results show that Ti_2AlC and Ti_2AlN exhibit metallic conductivity with an anisotropic character, i.e., the electrical conductivity is higher in the basal plane, whereas it is relatively lower along *c* axis. The chemical bonding in Ti_2AlC and Ti_2AlN are metallic-covalent-ionic in nature. The chemical bonding in the two hexagonal compounds also have an anisotropic character. An increase in covalent bonding was shown from Ti_2AlN to Ti_2AlC owing to the *sp* hybridization, on the contrary, a decrease in ionic and metallic bonding was illustrated. The high melting point and high modulus of these laminated materials are attributed to the strong Ti-C or Ti-N bonding, while the high electrical conductivity and microscale plasticity are attributed to the metallic bonding in the structure. Finally, we conclude on the basis of total-energy estimates that the replacement of C by N will result in a stabilization of the hexagonal lattice and decrease in metallic properties.

This work was supported by the National Outstanding Young Scientist Foundation under Grant No. 59925208, the National Science Foundation of China under Grant No. 59572013, Grant No. 59772021, and the 863 program.

---

[1] M. W. Baroum, D. Brodkin, and T. El-Raghy, Scr. Mater. **36**, 535 (1997).
[2] M. W. Barsoum and T. El-Raghy, J. Am. Ceram. Soc. **79**, 1953 (1996).
[3] Y. C. Zhou, Z. M. Sun, S. Q. Chen, and Y. Zhang, Mat. Res. Innovat. **2**, 142 (1998).
[4] Y. C. Zhou and Z. M. Sun, J. Appl. Phys. **86**, 1430 (1999).
[5] Z. M. Sun and Y. C. Zhou, Mat. Res. Innovat. **2**, 227 (1999).
[6] T. Goto and T. Hirai, Mater. Res. Bull. **22**, 1195 (1987).
[7] M. W. Barsoum and T. El-Raghy, Metall. Mater. Trans. A **30**, 363 (1999).
[8] Y. C. Zhou and Z. M. Sun, Mat. Res. Innovat. **2**, 360 (1999).
[9] P. Car and M. Parrinello, Phys. Rev. Lett. **55**, 2471 (1998).
[10] P. Hohenbery and W. Kohn, Phys. Rev. B **136**, 864 (1964).
[11] W. Kohn and L. J. Sham, Phys. Rev. **140**, A1133 (1965).
[12] J. P. Perdew and A. Zunger, Phys. Rev. B **23**, 5048 (1981).
[13] G. P. Kerker, J. Phys. C **13**, L189 (1980).
[14] L. Kleinman and D. M. Bylander, Phys. Rev. Lett. **48**, 1425 (1982).
[15] P. D. King-Smith, M. C. Payne, and J.-S. Lin, Phys. Rev. B **44**, 13 063 (1991).
[16] W. B. Person, Acta Crystallogr., Sect. A: Cryst. Phys., Diffr., Theor. Gen. Crystallogr. **A36**, 724 (1980).
[17] W. Jeitschko, H. Nowotny, and F. Benesovsky, Monatsch. Chem. **94**, 672 (1963).
[18] W. Jeitschko, H. Nowotny, and F. Benesovsky, Monatsch. Chem. **94**, 1198 (1963).